A Compact Dual-band Endfire Antenna with Balanced Microstrip Line Feed

Fang Wang, Runbo Ma, Liping Han, Rongcao Yang, and Wenmei Zhang,
College of Physics and Electronics, Shanxi University, Shanxi, 030006, China
e-mail:zhangwm@sxu.edu.).

Abstract—A dual-band endfire antenna with balanced microstrip line feed is proposed in this paper. The basic structure is a Yagi antenna composed of three microstrip dipoles. By introducing a dielectric layer and metallic layer under the basic Yagi antenna, the antenna realizes dual-band operation. Meanwhile, to broaden the bandwidth at 2.4 GHz, a parasitic slot is etched on the patch of the new metallic layer. The measured results indicate that the realized antenna operates in 2.4 and 5.2 GHz bands with the bandwidths of 780 MHz (2.31 GHz – 3.09 GHz) and 370 MHz (5.0 GHz – 5.37 GHz), covering the band for WLAN and WIFI. The maximum gains in the two bands are 1.4 dBi and 3.47 dBi, respectively.

Index Terms — **dual-band, endfire, Yagi antenna, parasitic slot.**

I. INTRODUCTION

IN recent years, RF energy harvesting technology has drawn great interests of researchers, since it provides an economical solution for battery life and replacement, making self sustainable devices feasible. RF energy harvesting systems require multiband antennas with high gain as RF signal receiver to improve input sensitivity. As a typical high gain antenna, the dual-band endfire antenna can be one of the feasible solutions. A dual-band (915 - 935 MHz and 1760 - 1805 MHz) Yagi-Uda antenna with branch structures was proposed in [1]. The elements of the antenna were constructed of brass wires, so it was not easy to integrate. In [2], a dual-band endfire antenna operating at 1.7 and 2.45 GHz with the bandwidth of 7% and 0.8% was achieved by adding the dipole element and the corresponding director element. In [3], a dual-band microstrip Yagi antenna including a double-dipole driver element was proposed. The realized antenna operated in 2.4 GHz and 5 GHz bands with the bandwidths of 4.4% and 20.36%, respectively. In [4], a dual-band quasi-Yagi monopole antenna was proposed. Two monopole drivers were used to determine the low (1.765 GHz) and high frequency (1.9 GHz). The realized bandwidths in two bands were 5.1% and 7.9%, respectively. The antenna had small sizes in comparison with the printed dual-band quasi-Yagi antennas with the dipole driver. In [5], a printed Yagi-Uda antenna with a meandered driven dipole and a concave parabolic reflector was proposed. The antenna achieved the dual-band operation by using a pair of strip lines to connect the driven dipole and its director. The novel antenna has the bandwidth of 4% and 6.5% at 1.58 and 2.645 GHz, respectively. In [6], a dual-band slot quasi-Yagi antenna was proposed for WLAN (2.4 GHz) and WIMAX (3.5 GHz) communication systems. Two modes (long- and short-slot mode) were generated simultaneously to realize the dual-band property and the bandwidth of 7.1% and 2.3% were obtained in two bands, respectively. In order to broaden the bandwidth, J. Liu et al etched three shunted dipoles in the ground plane and realized a novel dual-band quasi-Yagi antenna with 37.1% and 13.6% bandwidth at 2.4 and 5.5 GHz, respectively [7]. In this design, the dimension of the driver was smaller than the director, which was different from other microstrip Yagi antennas.

In this paper, a novel compact dual-band microstrip Yagi antenna with wider bandwidth in low band is presented to further reduce the area. To attain the dual-band radiation, a dielectric substrate and a metal patch are introduced. The metal patch is connected with the microstrip dipoles through a via-hole. Besides, by etching a parasitic slot on the metal patch, the bandwidth at lower frequency is broadened. The measured results show that the antenna can operate in 2.4 GHz and 5.2 GHz bands. The -10 dB relative bandwidths are 31% (2.31 GHz – 3.09 GHz) and 7.2% (5.0 GHz – 5.37 GHz), respectively. Furthermore, the maximum gains in the two bands are 1.4 dBi and 3.47 dBi, respectively.

II. STRUCTURE AND DESIGN OF ANTENNA

The proposed antenna is shown in Fig. 1. It consists of 2-layer substrates and 3-layer metals. The basic microstrip Yagi antenna is designed on the two sides of the top substrate (the top and bottom patches are denoted as the dark and light grey part, respectively). Its active dipole, director and microstrip feedline are symmetrically distributed on both sides of the dielectric layer. The reflector is on the top surface. Under the basic microstrip Yagi antenna, the second dielectric layer containing a rectangular patch is arranged to realize the dual-band operation. The rectangular patch is connected to the second metal layer through a via-hole and a parasitic slot is etched in it. The antenna is fabricated on a FR4-epoxy substrate with the thickness of 1.6 mm, the permittivity of 4.4 and dielectric loss tangent of 0.02. The total dimension of the two substrates is 78 mm × 43 mm and 78 mm × 39 mm, respectively. Fig. 2 shows the detailed parameters of the three metallic layers. Table I shows the optimized parameters of the proposed antenna.

TABLE I
STRUCTURAL PARAMETERS OF THE PROPOSED ANTENNA (UNIT: mm)

parameter	L_r	W_r	L	W	L_d	W_d	l_f	w_f
value	28.85	7	25	7	8.5	7	23	3
parameter	S_g	L_p	W_P	L_s	W_s	D_P	D_s	
value	1	68	14	34	1	2	7	

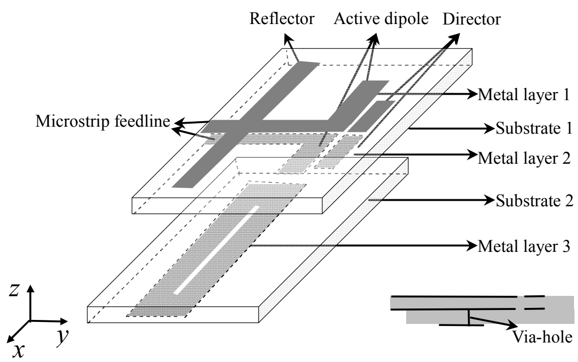

Fig. 1. Structure of the proposed antenna.

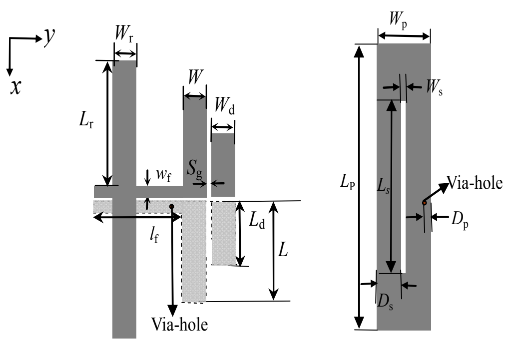

(a) (b)

Fig. 2. Schematics of the three layers of metal patches: (a) the first and the second metallic layers, (b) the third metallic layer.

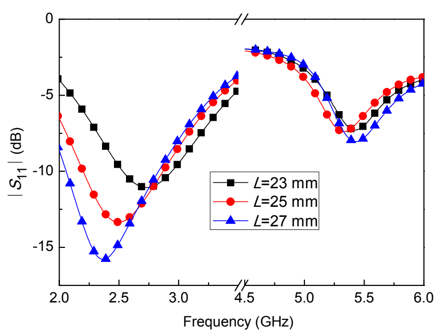

(a)

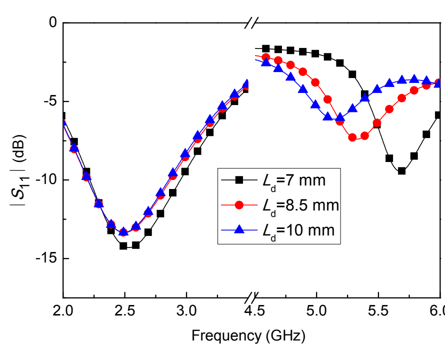

(b)

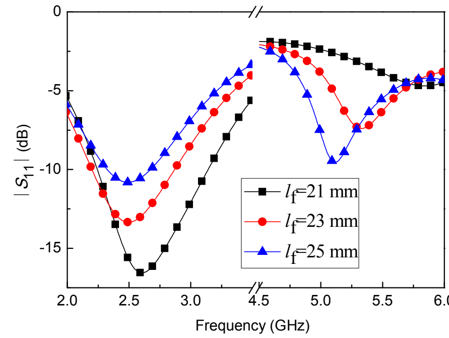

(c)

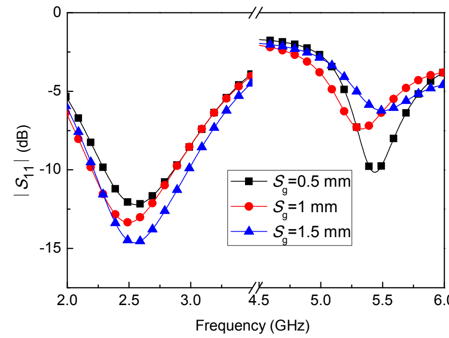

(d)

Fig. 3. Simulated $|S_{11}|$ for different parameters: (a) L, (b) L_d, (c) l_f, (d) S_g.

A. Parameter Analysis of the Basic Microstrip Yagi Antenna

In this section, the basic microstrip Yagi antenna is analyzed and the results are shown in Fig. 3. Fig. 3 (a) shows the influence of length L of the active dipole on $|S_{11}|$. It can be seen that the antenna resonates at around 2.4 GHz and 5.2 GHz. In 2.4 GHz band, the central frequency moves to lower frequency and $|S_{11}|$ decreases with the increase of L. In 5.2 GHz band, $|S_{11}|$ is larger than -10 dB and has less change with L. Fig. 3 (b) displays the influence of length L_d of the director on $|S_{11}|$. L_d mainly affects the performance in 5.2 GHz band. As L_d increases, the central frequency reduces and $|S_{11}|$ increases. This indicates that L_d becomes the radiating parts for the high band because of the offsets in the x and z directions between the metal layers 1 and 2. Fig. 3 (c) illustrates the influence of l_f on $|S_{11}|$. The central frequency reduces and $|S_{11}|$ shows opposite change with the increase of l_f in two bands. This reveals that l_f is also the radiating parts for the two bands. Fig. 3 (d) shows the influence of the gap S_g on $|S_{11}|$. S_g has little effect on the center frequency in lower band, but it mainly affects the $|S_{11}|$ in higher band. With the value of S_g increases, $|S_{11}|$ in higher band increases.

B. Influence of the Rectangular Patch

In order to achieve a good impedance matching in two bands, a dielectric layer and a metallic layer are introduced under the basic Yagi antenna analyzing in part A. Also, the metallic layer is connected to the microstrip dipoles through a via-hole. Fig. 4 illustrates the $|S_{11}|$ for different W_p, width of the rectangular patch. Before the rectangular patch is arranged (W_p = 0 mm), the antenna only operates in 2.4 GHz band. In 5.2 GHz band, $|S_{11}|$ is larger than -10 dB. After introducing a dielectric layer

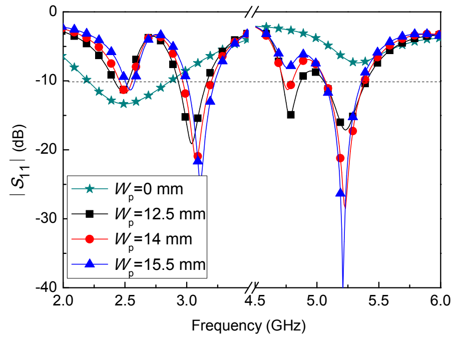

Fig. 4. Simulated $|S_{11}|$ for different W_{P}.

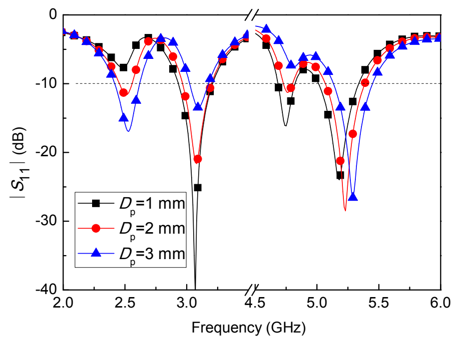

Fig. 5. Simulated $|S_{11}|$ for different D_{p}.

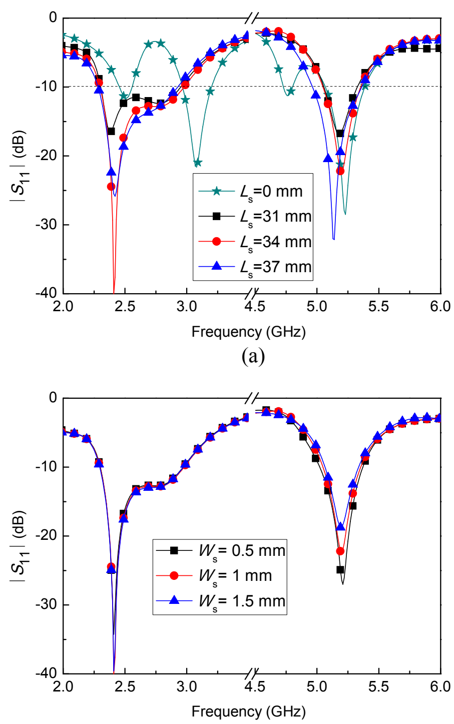

(a)

(b)

Fig. 6. Simulated $|S_{11}|$ for different parameters: (a) L_{s}, (b) W_{s}.

and a metallic layer, a new operating frequency band occurs at around 5.2 GHz. As the W_{p} increases, the central frequency in this band does not change and $|S_{11}|$ decreases gradually. But in 2.4 GHz band, the impedance bandwidth reduced largely. Fig. 5 illustrates the effect of the position of via-hole on $|S_{11}|$. It indicates that the position of via-hole mainly affects the $|S_{11}|$ in

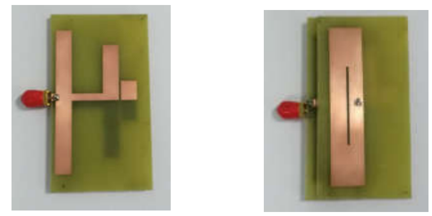

(a) (b)

Fig. 7. Photos of the proposed antenna: (a) the top view, (b) the bottom view.

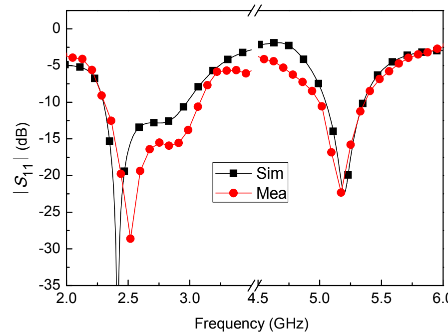

Fig. 8. Simulated and measured $|S_{11}|$.

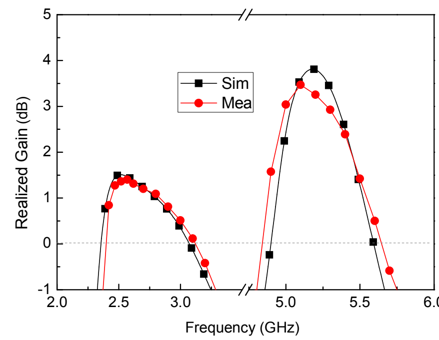

Fig. 9. Simulated and measured endfire gains.

2.4 GHz band and the central frequency in 5.2 GHz band. The central frequency in 5.2 GHz band moves to higher frequency slightly with the increase of D_{P}.

C. *Influence of the Parasitic Slot*

In Fig. 4, after the rectangular patch is arranged, the bandwidth in 2.4 GHz band is reduced. To improve it, a parasitic slot is etched on the patch of third metallic layer which is introduced in part B. Fig. 6 gives the effect of the length L_{s} and width W_{s} of the slot on $|S_{11}|$, respectively. In Fig. 6 (a), for the antenna without the slot, it has a relative bandwidth of 4.4% (from 2.45 GHz to 2.56 GHz) in 2.4GHz band. After the slot is etched on the rectangular patch, another resonant frequency appears near the 2.4 GHz and the bandwidth is improved largely. When $L_{\mathrm{s}} = 34$ mm, the maximum relative bandwidth of 28.3% (from 2.3 GHz to 2.98 GHz) is obtained. Meanwhile, the bandwidth barely changes in 5.2 GHz band. Fig. 6 (b) shows the effect of the W_{s} on $|S_{11}|$. With the increase of W_{s}, the center frequency in two bands has no change and the $|S_{11}|$ in 5.2 GHz band increases. Also, the bandwidth in 5.2 GHz band reduces a little. Finally, we select $W_{\mathrm{s}} = 1$ mm because it is easier to implement than 0.5 mm.

III. Simulated and Measured Results

To validate the design concept, a prototype of the proposed microstrip Yagi antenna is fabricated and the photos are shown in Fig. 7. The Agilent N5230A vector network analyzer and antenna training and measuring system 8092 (Lab-Volt corporation) are used to measure the antenna. The measured results are shown in Figs. 8-11.

Fig. 8 shows the simulated and measured $|S_{11}|$. The simulated central frequencies are 2.4 GHz and 5.2 GHz and the corresponding operating bandwidths are 2.3 - 2.98 GHz and 5.05 - 5.35 GHz, respectively. The measured central frequencies are 2.52 GHz and 5.17 GHz and the corresponding operating bandwidths are 31% (2.31 - 3.09 GHz) and 7.2% (5.0 - 5.37 GHz), respectively. The measured results are in good agreement with the simulated results. Fig. 9 gives the simulated and measured endfire gains versus frequencies. The simulated maximum gains are 1.5 dBi and 3.8 dBi, and the measured ones are 1.4 dBi and 3.47 dBi in the two bands, respectively.

Figs. 10 and 11 illustrate the simulated and measured E-plane and H-plane radiation patterns at 2.4 GHz and 5.2 GHz. It can be seen that the acceptable endfire radiation patterns have been obtained. Note that the antenna offers a front-to-back ratio of 10 dB. Additionally, the broadside half-power beamwidths (HPBW) have been observed at both frequencies. Moreover, it can be observed that there is a larger sidelobe in E-plane radiation pattern at 5.2 GHz.

Finally, Table II lists the key data of this work and those reported dual-band Yagi antennas. Compared with Refs. [1]-[6], the proposed endfire antenna has the smaller dimension and achieves the wider relative bandwidth in lower band.

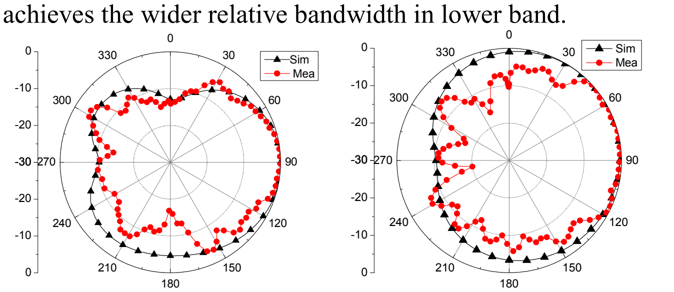

(a) (b)

Fig. 10. Radiation patterns at 2.4 GHz. (a) E-plane, (b) H-plane.

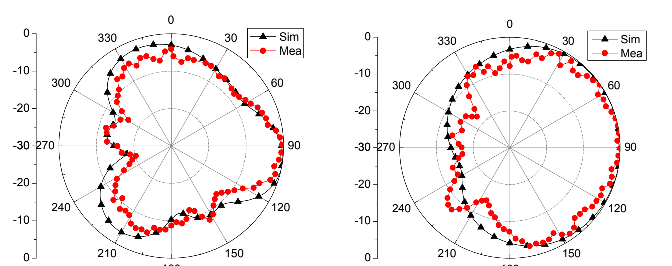

(a) (b)

Fig. 11. Radiation patterns at 5.2 GHz. (a) E-plane, (b) H-plane.

IV. Conclusion

This letter presents a new type of dual-band endfire antenna. The antenna realizes the dual-band radiation by introducing a dielectric layer and a metallic layer under the basic microstrip Yagi antenna. Also, the bandwidth in the lower band is broadened by etching a parasitic slot on the metal patch. The measured results show that the antenna can operate at 2.4 GHz and 5.2 GHz bands with the relative bandwidths of 31% (2.31 GHz – 3.09 GHz) and 7.2% (5.0 GHz – 5.37 GHz), respectively. Furthermore, the maximum gains in the two bands are 1.4 dBi and 3.47 dBi, respectively. The further work is to improve the bandwidth in the higher band by modifying the construction of the introduced rectangular patch.

TABLE II
Performance of Dual-Band Yagi Antennas

Ref.	Size (mm^3)	Antenna structures	f_L/f_H (GHz)	RB_L/RB_H (%)	The Max. gain (dBi)
[1]	163×158.7×2.2	3D	0.92/1.782	2.2/2.5	6/6.6
[2]	120×80×1.5	one-layer	1.7/2.45	7.0/0.8	⁄
[3]	33×52×0.8	one-layer	2.45/5.5	4.4/20.36	4.4/5.8
[4]	80×40×1.5	one-layer	1.76/1.9	5.1/7.9	⁄
[5]	68×54.5×0.8	one-layer	1.58/2.645	4.0/6.5	6.7/4.9
[6]	65×61×11.6	3D	2.4/3.5	7.1/2.3	8.14/9.43
[7]	116×56×0.8	one-layer	2.4/5.5	37.1/13.6	5.0/5.3
This work	78×43×3.2	two-layers	2.4/5.2	31/7.2	1.4/3.47

f_L and f_H are center frequency in the low and high band, respectively. RB_L and RB_H are the relative bandwidth in the low and high band, respectively.

Acknowledgment

This work was supported by the National Science Foundation of China (61771295 61775126)

References

[1] Q. Xin, F. Zhang, B. Sun, Y. Zou, and Q. Liu, “A Novel Dual-band Yagi-Uda Antenna for Wireless Communications,” in *Proc. IEEE 9th ISAPE*, 2010, pp. 289–292.

[2] A. P. Gorbachev and N. V. Tarasenko, “The Modified Dual-frequency Quasi-Yagi Antenna,” in *Proc. IEEE 15th Int. Conf. on EDM*, 2014, pp. 161–163.

[3] Y. Zhang and Z. Li, “A Dual-band Planar Quasi-Yagi Antenna with Double-dipole Driver,” in *Proc. IEEE 6th Int. Symp. on MAPE*, 2015, pp. 123–125.

[4] N. V. Tarasenko, “Investigation of the Printed Dual-band Quasi-Yagi Monopole Antenna Matching,” in *Proc. IEEE Int. Conf. on APEIE*, 2014, pp. 403–405.

[5] H. Huang, J. Lu, and P. Hsu, “A Compact Dual-band Printed Yagi-Uda Antenna for GNSS and CMMB Applications,” *IEEE Trans. Antennas Propag*., vol. 63, no. 5, pp. 2342-2348, 2015.

[6] H. Liu, Y. Liu, and S. Gong, “A Dual-band Slot Quasi-Yagi Monopole Antenna with Very Low Profile,” in *Proc. IEEE ISAP*, 2015.

[7] D. Chang, C. Chang, and J. Liu, “Modified Planar Quasi-Yagi Antenna for WLAN Dual-band Operations,” *Microw. Opt. Technol. Lett*., vol. 46, no. 5, pp. 443-446, 2005.